Heliyon 10 (2024) e38661

Contents lists available at ScienceDirect

Heliyon

journal homepage: www.cell.com/heliyon

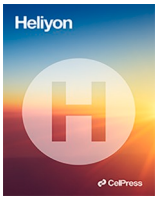

Research article

Exogenous hydrogen sulfide enhances myogenic differentiation of C2C12 myoblasts under high palmitate stress

Fangping Lu [a,c,1], Shiwu Zhang [a,1], Shiyun Dong [a,1], Mengyi Wang [a], Kemiao Pang [a], Yajun Zhao [a], Jiayi Huang [a], Jiaxin Kang [a], Ning Liu [a], Xueya Zhang [a], Dechao Zhao [b,**], Fanghao Lu [a,***], Weihua Zhang [a,*]

[a] Department of Pathophysiology, Harbin Medical University, Harbin, China
[b] Department of Cardiology, First Affiliated Hospital of Harbin Medical University, Harbin, China
[c] Department of Pathophysiology, Mudanjiang Medical University, Mudanjiang, China

ARTICLE INFO

Keywords:
Hydrogen sulfide
Type 2 diabetes
Skeletal muscle atrophy
Myoblast differentiation
MuRF1

ABSTRACT

Skeletal muscle atrophy was one of main complications of type 2 diabetes mellitus. Hydrogen sulfide (H_2S) is involved in various physiological functions, such as anti-hypertension and anti-oxidant. Skeletal muscle atrophy caused by type 2 diabetes could lead to the regeneration of muscle fibers. Wnt signaling pathway plays a crucial important role in this process. H_2S maybe regulate the Wnt signaling pathway to alleviate skeletal muscle atrophy, however, this role has not been clarified. The aim of this study is to investigate the potential regulatory role of H_2S in the Wnt signaling pathway. C2C12 myoblasts treated with 500 μmol palmitate as an in vitro model. Western blot was used to detect the levels of CSE, PKM1, β-catenin, MuRF1, MYOG, MYF6 and MYOD1. In addition, MuRF1 was mutated at Cys44 and MuRF1 S-sulfhydration was detected by biotin switch assay. The interaction between PKM1 and MuRF1 was assessed via Co-immunoprecipitation. Differentiation of C2C12 myoblasts was evaluated using LAMININ staining. These data showed the levels of CSE, β-catenin, PKM1, MYOG, MYF6 and MYOD1 were decreased in pal group, compared with control and pal + NaHS groups. MuRF1 Cys44 mutants increased the protein levels of β-catenin, MYOG, MYF6 and MYOD1 in pal group. Our results suggest that H_2S regulates the S-sulfhydration levels of MuRF1 at Cys44, influencing the ubiquitination levels of PKM1 and ultimately promoting myoblast differentiation.

1. Introduction

Diabetes mellitus (DM), as a metabolic disease, is known to lead to skeletal muscle atrophy [1], which significantly impacts the quality of life for affected individuals. Excessive oxidative stress plays a central role in the progression of Type 2 Diabetes (T2DM), as antioxidant defense systems are impaired in T2DM patients [2]. Skeletal muscle, responsible for 80 % of insulin-stimulated glucose uptake, efficiently regenerates via satellite cells, aiding in maintenance, growth, repair, and post-birth regeneration [3]. Muscle

* Corresponding author.
** Corresponding author.
*** Corresponding author.
E-mail addresses: drzhaodechao@163.com (D. Zhao), lufanghao1973@126.com (F. Lu), zhangwh116@126.com (W. Zhang).
[1] These authors contributed equally to this work.

https://doi.org/10.1016/j.heliyon.2024.e38661
Received 26 June 2024; Received in revised form 3 September 2024; Accepted 26 September 2024
Available online 27 September 2024

damage activates satellite cells. Myoblasts either differentiate, contributing to muscle repair, or return to a quiescent state to sustain the stem cell pool [4,5]. Both quiescent and activated satellite cells express the characteristic marker Pax7, whereas myogenic regulatory factors Myf5 (Myogenic factor 5) and MyoD (Myogenic determination factor) are expressed by activated satellite cells [6]. It has been reported that satellite cell proliferation is reduced, and muscle regeneration is impaired in ob/ob and db/db mice [7], but the underlying mechanisms remain unclear.

Wnt signaling directs stem cell fate by controlling β-catenin. Phosphorylation inactivates β-catenin, but when unphosphorylated, it enters the nucleus, forming complexes with TCF and LEF. This triggers the activation of target genes like MYOG and MYOD, influencing stem cell differentiation [8,9]. Canonical Wnt signaling plays a crucial role in regulating the activity of myogenic regulatory factors during myogenic differentiation [10]. β-catenin can undergo post-translational modifications, such as phosphorylation and acetylation. P300/CBP-associated factor (PCAF) activates β-catenin by competing with ubiquitination sites on Lys-19 and Lys-49, preventing its ubiquitination and degradation [11]. Pyruvate, derived from glucose, is enzymatically converted by the pyruvate dehydrogenase complex into acetyl-CoA. This acetyl-CoA is then transported from mitochondria to the cytoplasm via the citrate carrier (CIC) [12], where it is reconverted to acetyl-CoA by adenosine triphosphate citrate lyase (ACLY) [13]. Subsequently, acetyl-CoA is used for protein acetylation.

Muscle-specific RING finger protein 1 (MuRF1), also known as TRIM63, is a ring-type E3 ligase, and MuRF1 belongs to the RING-B-box-coiled-coil (RBCC) or tripartite motif (TRIM) family. MuRF1 extensively expresses in cardiac muscle and skeletal muscle. Given MuRF1's involvement in muscle atrophy, our previous study confirmed an upregulation of MuRF1 expression in db/db mice [14]. MuRF1 consists of an RBCC motif comprising a RING domain, B-box type 2 domain, COS-box domain with a central helical domain, and a C-terminal acidic tail [15].

Hydrogen sulfide is a gaseous molecule with a broad spectrum of physiological functions, encompassing the regulation of vasodilation, modulation of lipid metabolism, induction of angiogenesis, and antioxidative effects [16–21]. Enzymatic H_2S production, on the other hand, is primarily mediated by three enzymes: cystathionine-β-synthase (CBS), cystathionine-γ-synthase (CSE), and 3-Mercaptopyruvate sulfurtransferase (3-MST) [22,23]. H_2S can induce S-sulfhydration modifications on cysteine residues within target proteins [24], converting the sulfhydryl group on cysteine sites into -SSH groups, thereby increasing the reactivity of the cysteine amino group. In this study, we investigated how H_2S modified MuRF1 through S-sulfhydration and its regulatory role in myoblast differentiation.

2. Materials and methods

2.1. Materials

Leptin receptor knockout db/db mice purchased from Nanjing Experimental Animal Center were used as an experimental animal model for type 2 diabetes. 80 db/db mice and 50 C57/BL mice were placed in a suitable environment. If the blood glucose was measured for 3 consecutive days >16.7 mmol/L, the model was considered successful, and the db/db mice were randomly divided into two groups, the db/db group (n = 40) and the other part of the mice received intraperitoneal injection of NaHS (4.8 mg/kg, once every other day). Raised for 20 weeks, during this period, blood glucose and glucose tolerance tests were carried out once a week to ensure the accuracy of modeling. The gastrocnemius muscle of mice was taken for measurement. Some of them were fixed with 4 % paraformaldehyde for subsequent fluorescence experiments. After extraction with liquid nitrogen, the remaining tissue was frozen at −80 °C for protein content detection. All animal care and experimental design were approved by the Harbin Medical University Medical Science Ethics Committee (Approval No. HMUIRB2022015).

2.2. Cellular experimental protocol

C2C12 myoblasts were cultured with Gibco high-glucose medium containing 10 % fetal bovine serum, and the cells were subcultured when their density grew to about 80 % or more. The subcultured cells were placed in Gibco high-glucose medium containing 10 % fetal bovine serum. When the cells growth density reached 70 %–80 %, they could be randomly divided into control group (Control, DMEM), pal (pal, 500 μmol/L), pal + NaHS (NaHS, 100 μmol/L), pal + NaHS + PPG (DL-propargylglycine, CSE inhibitor, 10 nmol/L), Control + DTT (Dithiothreitol, inhibitor of disulfide bonds, 10 nmol/L), pal + DTT (Dithiothreitol, inhibitor of disulfide bonds, 10 nmol/L), pal + NaHS + DTT (Dithiothreitol, inhibitor of disulfide bonds, 10 nmol/L), pal + N-acetylcysteine (NAC, ROS scavenger, 100 μmol/L), pal + 4-phenylbutyrate (4-PBA, ER stress inhibitor, 5 mmol/L), Control + thapsigargin (Tg, ER stress inducer, 100 μmol/L), pal + MG132 (26S proteasome inhibitor, 20 μmol/L), pal + NaHS + C646 (histone acetyltransferase P300 inhibitor, 10 μmol/L), pal + NaHS + SB204990 (ATP citrate lyase acly specific inhibitor, 100 μmol/L). After 48 h or 12 h of treatment, C2C12 myoblasts were treated with 2 % horse serum for 4 days, and the cells were collected.

The primary skeletal muscle satellite cells (SC) used in our in vitro experiments were derived from muscle biopsies from the hindlimbs of adult mice. Mouse skeletal muscle primary satellite cells were cultured in complete medium (basal medium containing 10 % fetal bovine serum, 1 % supplements, and 1 % double antibody). When the density reached 70 %–80 %, they were randomly divided into control group (Control, DMEM), pal (pal, 500 μmol/L), pal + NaHS (NaHS, 100 μmol/L), pal + NaHS + PPG (DL-propargylglycine, CSE inhibitor, 10 nmol/L), pal + N-acetylcysteine (NAC, ROS scavenger, 100 μmol/L), the cells were collected.

2.3. Co-immunoprecipitation experiments

Diluted the protein concentration of the cells in each group to 2 μg/μL, and added 20 μl of IgG agarose magnetic beads to 1 ml of the sample. The magnetic beads and the EP tube of the protein sample were rotated and incubated for 30 min, then removed and centrifuged at 10000 g at 4 °C for 3 min. IgG Sepharose Magnetic Beads (1:20) mixed well and incubated overnight with continued rotation. For the ubiquitination assay, anti-ubiquitin (PTM) (2 μg of antibody was used per sample.) was used as the IP antibody. The next day, discarded the supernatant, resuspended the pellet with the prepared tissue lysate. Added lysis buffer and 4 × loading buffer to the pellet, and then Western blot was used to detect between protein and protein interactions.

2.4. Western blot

We used RIPA splitting buffer containing 1 mM PMSF to split C2C12 myoblasts and satellite cells to extract protein. Used BCA protein quantitative kit to detect protein concentration. After the sodium dodecyl sulfate (SDS)-polyacrylamide gel electrophoresis gel, the membrane transfer experiment was carried out. Put the NC membranes into the antibody diluted with TBST, and incubated membranes overnight. Anti-CSE, anti-TMP3, anti-TNNI2, anti-SOD, anti-CAT, anti-MYOD1, anti-PGC1α, anti-MYF6, anti-β-catenin, anti-β-Tubulin, anti-PKM1 and anti-MuRF1were from Proteintech. All antibodies were used at a 1:1000 dilution. The next day, continued to incubate the NC membrane with the prepared secondary antibody labeled with horseradish peroxidase at room temperature. The ECL color development was incubated on the NC membranes, and observed by a chemiluminometer, and photographs were taken for subsequent analysis of the gray value of the protein bands.

2.5. SOD, CAT activity detection

SOD and CAT activity detection kits were purchased from Solarbio Technology and Jice testing company, operated according to the instructions, used a spectrophotometer to detect the absorbance value, and finally calculated the activity of each histone sample.

2.6. Pyruvate (PA) content detection

The pyruvate content detection kit purchased from Solarbio Technology was operated according to the instructions, and the absorbance value of each group of samples at a wavelength of 520 nm was detected by microplate reader, and finally the pyruvate content of each group of samples was calculated.

2.7. Detection of intracellular ROS levels

C2C12 cells were treated with control, Pal, Pal + NaHS, Pal + NAC, Pal + PPG for 48 h. DHE (25 μmol/L) was prepared with serum-free DMEM, and incubated at 37 °C for 30 min in the dark. And then prepared Hoechst with serum-free DMEM, and incubated at room temperature for 10 min in the dark. The differences in ROS levels of each group of samples were observed under a fluorescence microscope and photographed. The intensity was analyzed by Image J.

2.8. Detection of intracellular H_2S levels

The cells were treated with drugs according to the experiment, 7-Azido-4-Methylcoumarin (C-7Az, 50 μmol/L) was prepared with serum-free DMEM and incubated at 37 °C for 30 min in the dark. The differences in the H_2S levels of each group of samples were observed under a fluorescence microscope and photographed.

2.9. Cellular immunofluorescence assay

The cells on the slides were fixed with 4 % paraformaldehyde for 30 min. Cells were permeabilized for 30 min with permeabilization solution (0.1 g of sodium citrate was dissolved in 100 ml of distilled water, and after it was fully dissolved, 100 μl of Triton was added). Blocked with 3 % BSA (0.3 g BSA in 10 ml of PBS) for 30 min. Diluted the primary antibody with 1 % BSA (0.1 g BSA plus 10 ml PBS) according to the needs of the experiment, and incubated at 4 °C overnight. The next day, the secondary antibody was diluted with 1 % BSA (0.1 g BSA in 10 ml of PBS), incubated at room temperature for 1 h. DAPI dye was added dropwise to the slides, incubated at room temperature for 5 min. And then took pictures with a fluorescence microscope.

2.10. Detection of intracellular S-sulfhydration levels

The cells were processed, the S-sulfhydration-specific fluorescent probe SSP4 (50 μmol/L) was prepared with serum-free DMEM, and incubated in the dark for 15 min. The differences in S-sulfhydration levels of each group of samples were observed with a microscope and photographed.

2.11. Detection of S-sulfhydration modified protein

The treated cells were scraped off and lysis buffer were added (HEN buffer contains Hepes-NaOH (250 mmol/L, pH adjusted to 7.7), EDTA (1 mmol/L)), Neocuproine (0.1 mmol/L) and Deferoxamine (100 mmol/L) were added to HEN buffer solution with 0.5 % (w/v) CHAPS, 0.1 % (w/v) SDS, 10 μg/mL Leupetin, 5 μg/mL Aprotinin, 1 mM PMSF) by vortexing for 30 min, the concentration of each group of samples was detected with BCA quantitative kit, and the concentration was diluted to 5 μg/μL. Took 200 μL of the diluted protein sample, added 4 times the volume of loading buffer (2.5 % (w/v) SDS, 20 mmol/L MMTS in HEN buffer) and incubated at 50 °C for 20 min. The remaining diluted samples were added to 4 × loading buffer, and the samples were boiled at 100 °C for 10 min. Added 4 vol of cold acetone to the incubated cells, incubated at −20 °C for 1 h, then at 4 °C, 2000 g for 10 min, removed the supernatant after

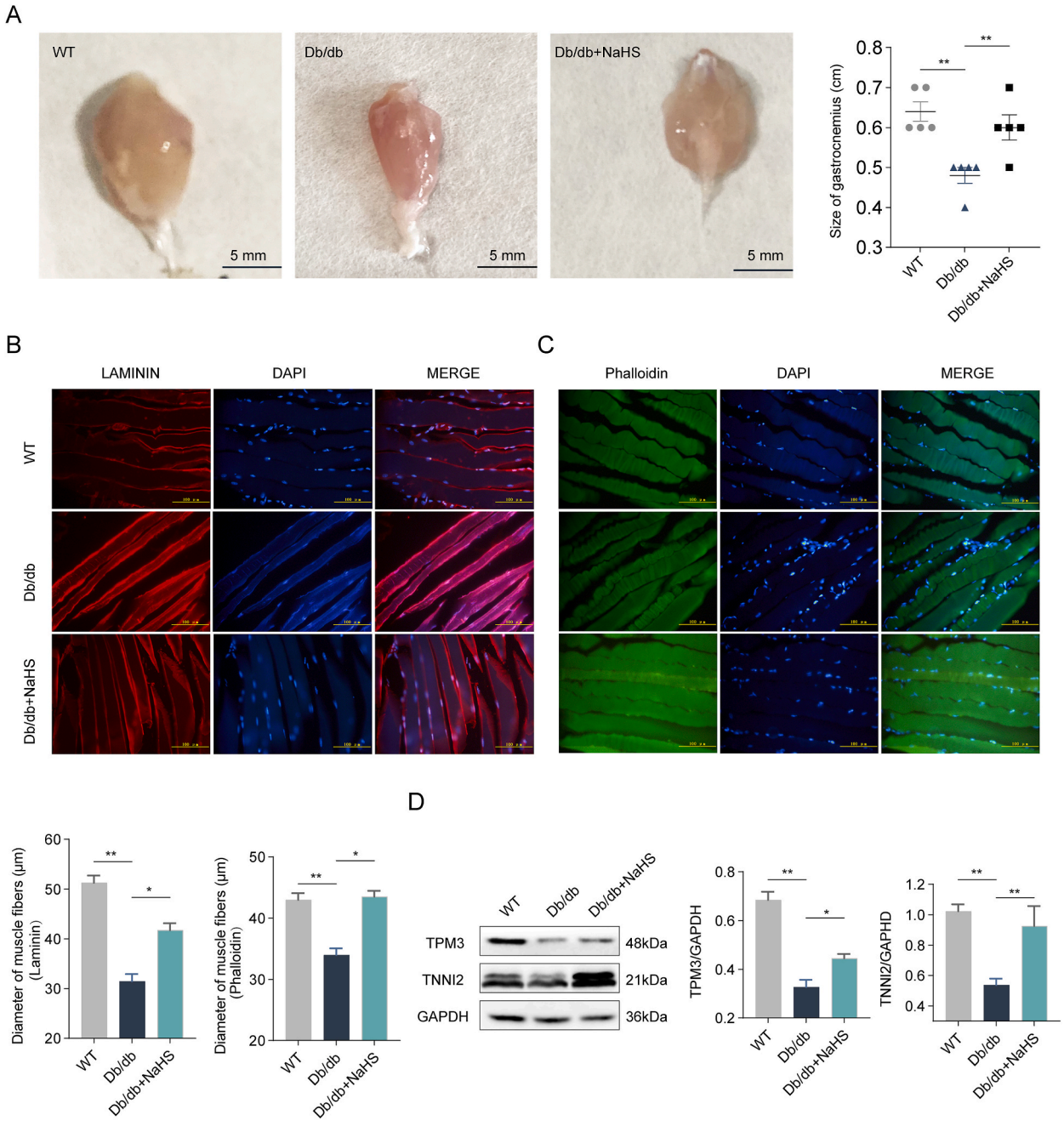

Fig. 1. Effect of exogenous H_2S on skeletal muscle atrophy in db/db mice at 20 w. (A) The diameter of gastrocnemius was measured. The scale bar: 0.5 cm. n = 5. (B) LAMININ staining was used to detect skeletal muscle atrophy. n = 5. (C) Phalloidin staining was used to detect skeletal muscle atrophy. n = 5. (D) The expression of skeletal muscle structural protein was detected by Western blot. n = 4.

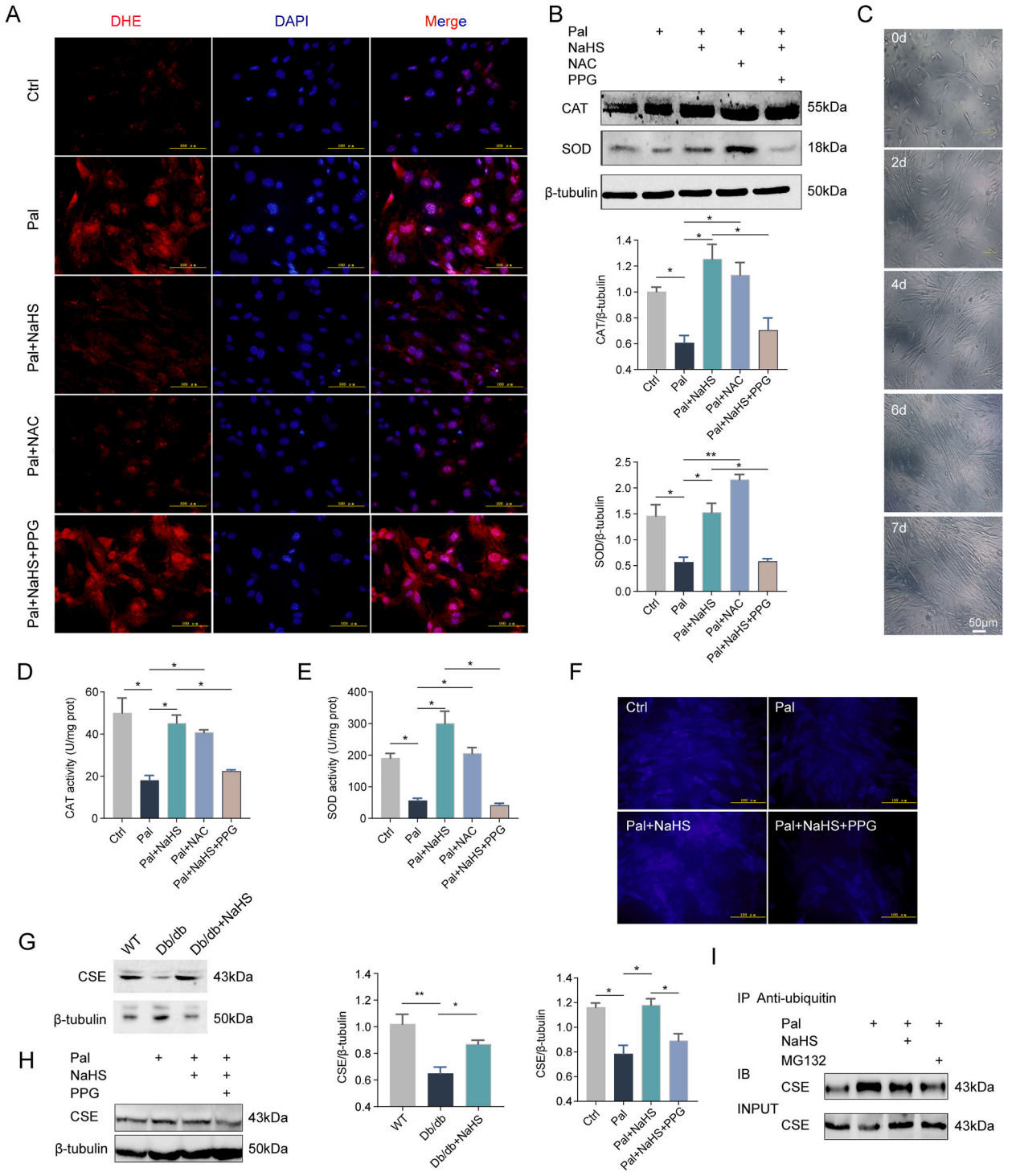

Fig. 2. Changes of oxidative stress related indexes of satellite cells and C2C12 myoblasts under pal state. (A) ROS production was detected by DHE probe staining. (B) The expression levels of SOD and CAT were detected by Western blot. n = 5. (C) C2C12 myoblasts differentiated. (D–E) The activities of SOD and CAT were detected by kit. n = 3. *P < 0.05, **P < 0.01, ***P < 0.001. (F) H2S specific probe staining. (G, H) The expression levels of CSE protein were detected by Western blot. n = 4. (I) The interaction between CSE and ubiquitin was detected by Co-immunoprecipitation experiment. *P < 0.05.

centrifugation, and dried the pellet. Added 90 μL of HEN buffer solution, resuspend the cells and transferred them to a labeled EP tube, added 10 μL of 15 mM biotin-HPDP stop solution to the EP tube, and incubated at room temperature for 1 h. Added 2 times volume of HEN buffer containing 20 μL of streptomycin affinity table agarose beads to the EP tube, incubated at 37 °C for 1 h, and shook slightly during this period. Washed the agarose beads 5 times with PBS, and used the eluent containing mercaptoethanol to elute the protein from the beads, incubated at 37 °C for 20 min, added native 4 × loading buffer, and used sample cooker at 95 °C for 5 min. The S-sulfhydration modification among each group of samples was detected by Western blot using an anti-MuRF1 antibody (Proteintech).

2.12. LC-MS/MS

Cell proteins were extracted using a lysis buffer with sonication, followed by centrifugation to remove debris, and protein concentration was determined using a BCA kit. The extracted proteins were then precipitated with acetone, reduced, alkylated, and digested with trypsin. The resulting peptides were desalted and analyzed via LC-MS/MS on a NanoElute UHPLC system coupled to a timsTOF Pro mass spectrometer, using a specified gradient for peptide separation. The data were processed with MaxQuant, searching against the Mus_musculus database, with strict criteria for protein identification, including a false discovery rate of less than 1 %.

2.13. Construction of MuRF1 mutants

The adenovirus expressing GFP and mouse MuRF1-GFP (non-fusion GFP-tagged) from Cyagen Biosciences, Guangzhou, China was purchased, the Cysteine (Cys) at site 44 in the mouse full-length MuRF1 protein sequence was mutated to alanine (Ala), and the GFP cDNA fragment was inserted into the PM vector (Cyagen Biosciences) between Kozak and T2A. When the cells grew to about 70 %, MuRF1 mutants with adenovirus were added to the culture medium for incubating C2C12 cells, incubated for 6 h, and replaced with fresh culture medium for 24 h. Cells treatment were continued according to the needs of the experiment. Finally, the protein content among each group of samples was detected by Western blot.

2.14. Statistical analysis

The experimental data was expressed as mean ± standard deviation (x ± s), and the comparison between the means of multiple samples was performed by analysis of variance. The diameter of the gastrocnemius muscle fibers was measured using a calibrated ruler. $P < 0.05$ has statistical significance, $P < 0.01$ has significant statistical significance, $P < 0.01$ has extremely significant statistical significance.

3. Results

3.1. Db/db mice caused gastrocnemius muscle atrophy

As anticipated, in line with previous research [14], our investigation revealed evident atrophy in the gastrocnemius muscle of db/db mice. The gastrocnemius muscle from 20-week-old db/db mice was isolated and quantified, revealing a discernible reduction in muscle size compared to the control group. Remarkably, administration of exogenous hydrogen sulfide (H_2S) demonstrated a notable attenuation of gastrocnemius muscle atrophy, as depicted in Fig. 1A. Immunostaining with LAMININ and Phalloidin (Fig. 1B and C) further corroborated the observation of gastrocnemius muscle atrophy in db/db mice, with the added revelation that H_2S treatment ameliorated this skeletal muscle atrophy. Additionally, as presented in Fig. 1D, the protein levels of TPM3 and TNNI2 were found to be diminished in db/db mice, yet the introduction of exogenous H_2S significantly augmented the expression of these proteins. Consequently, our findings substantiate the presence of gastrocnemius muscle atrophy in type 2 diabetic mice and underscore the therapeutic potential of exogenous H_2S in mitigating this skeletal muscle atrophy.

When satellite cells are subjected to external stimuli, they undergo a sequence of events involving proliferation, differentiation, fusion, ultimately culminating in the formation of muscle fibers, as depicted in Fig. S1A. Upon exposure to 10 % horse serum, satellite cells commenced differentiation into muscle fibers by day 4. In response to muscle injury, satellite cells were activated, co-expressing PAX7 and MYOD. To simulate the type 2 diabetes microenvironment, satellite cells were treated with 500 μM palmitate, and PAX7 staining was employed as a marker for satellite cells. BrdU staining was used to assess satellite cell proliferation, although discernible proliferation differences were not readily apparent among the groups (Fig. S1B).

3.2. Exogenous H_2S attenuated oxidative stress production in satellite cells and C2C12 myoblasts

The association between skeletal muscle atrophy in type 2 diabetes and oxidative stress has been well-established in previous research [14]. In vitro studies have highlighted the detrimental impact of hydrogen peroxide (H_2O_2) on human satellite cells, diminishing their lifespan and proliferative capacity [25]. These findings underscore the role of oxidative stress in impairing muscle regeneration within a diabetic context. To assess oxidative stress, we employed DHE staining to measure superoxide anion levels. In comparison to the control group, the palmitate-treated (pal) group exhibited heightened fluorescence intensity, whereas this intensity was restored following the administration of exogenous H_2S and NAC, but the fluorescence intensity was enhanced after with the treatment of PPG (inhibitor of CSE, 10 nmol/L) (Fig. 2A). Furthermore, a significant reduction in protein levels of SOD and CAT was observed in both the pal and pal + NaHS + PPG groups, in contrast to the control group (Fig. 2B). These results collectively indicate the

occurrence of oxidative stress in satellite cells under palmitate treatment, with exogenous H_2S emerging as an effective mitigator of this oxidative stress.

Satellite cells play a pivotal role in muscle regeneration, transitioning into myoblasts, which subsequently differentiate into muscle fibers. Although satellite cells and C2C12 myoblasts are distinct cell types, C2C12 myoblasts retain some satellite cell characteristics. Remarkably, our observations revealed the development of discernible muscle fibers in C2C12 myoblasts on the 4th day of differentiation under 2 % horse serum treatment (Fig. 2C). Our research, therefore, leveraged C2C12 myoblasts as a surrogate for satellite

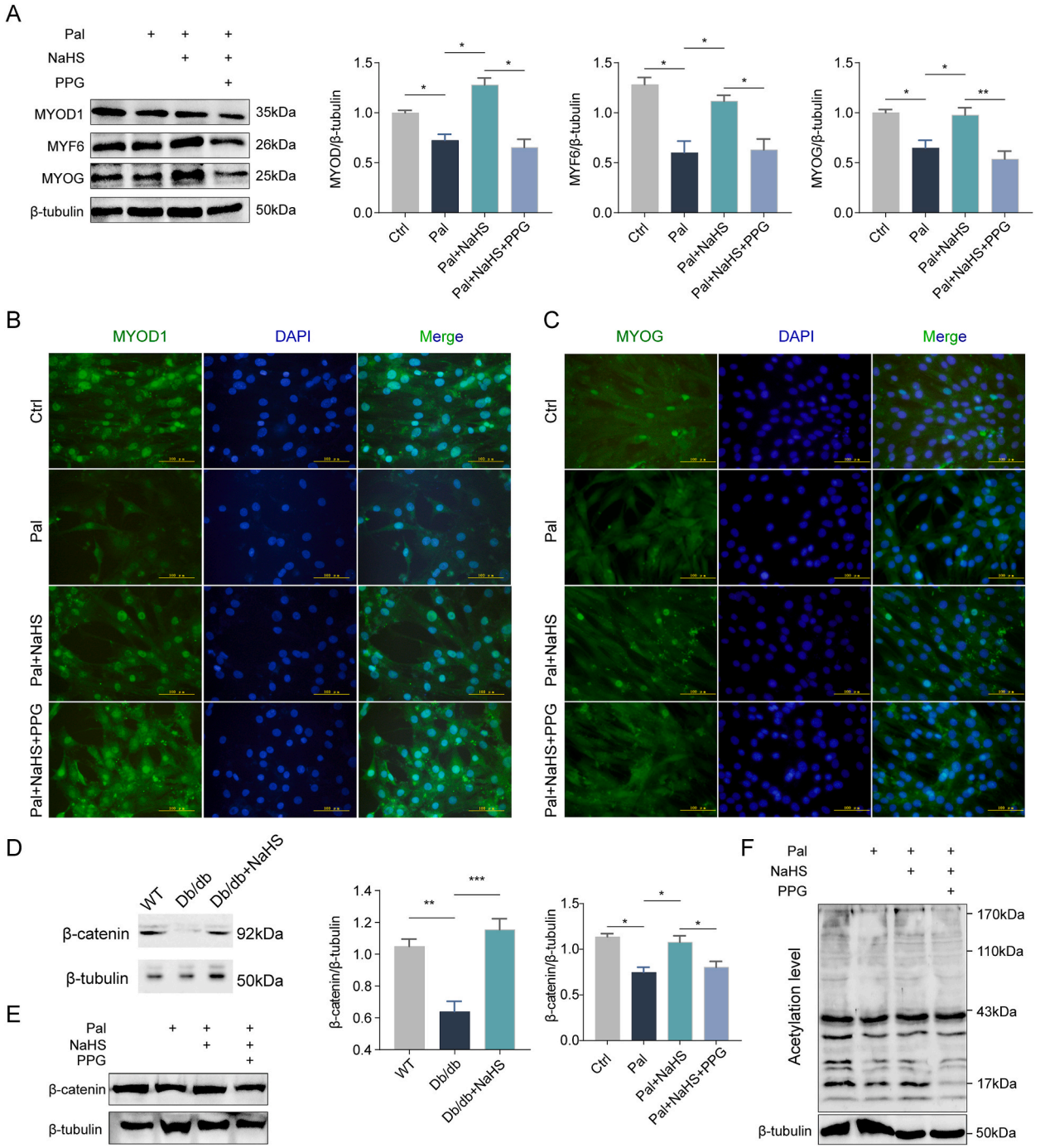

Fig. 3. Myogenic regulatory factors were detected in high palmitate state. (A) Myogenic regulatory factors were detected by Western blot. n = 5. (B–C) Immunofluorescence of MYOD1 and MYOG. (D, E) Western blot was used to detect the levels of β-catenin. n = 5. (F) The total acetylation levels were detected by Western blot. *P < 0.05, **P < 0.01.

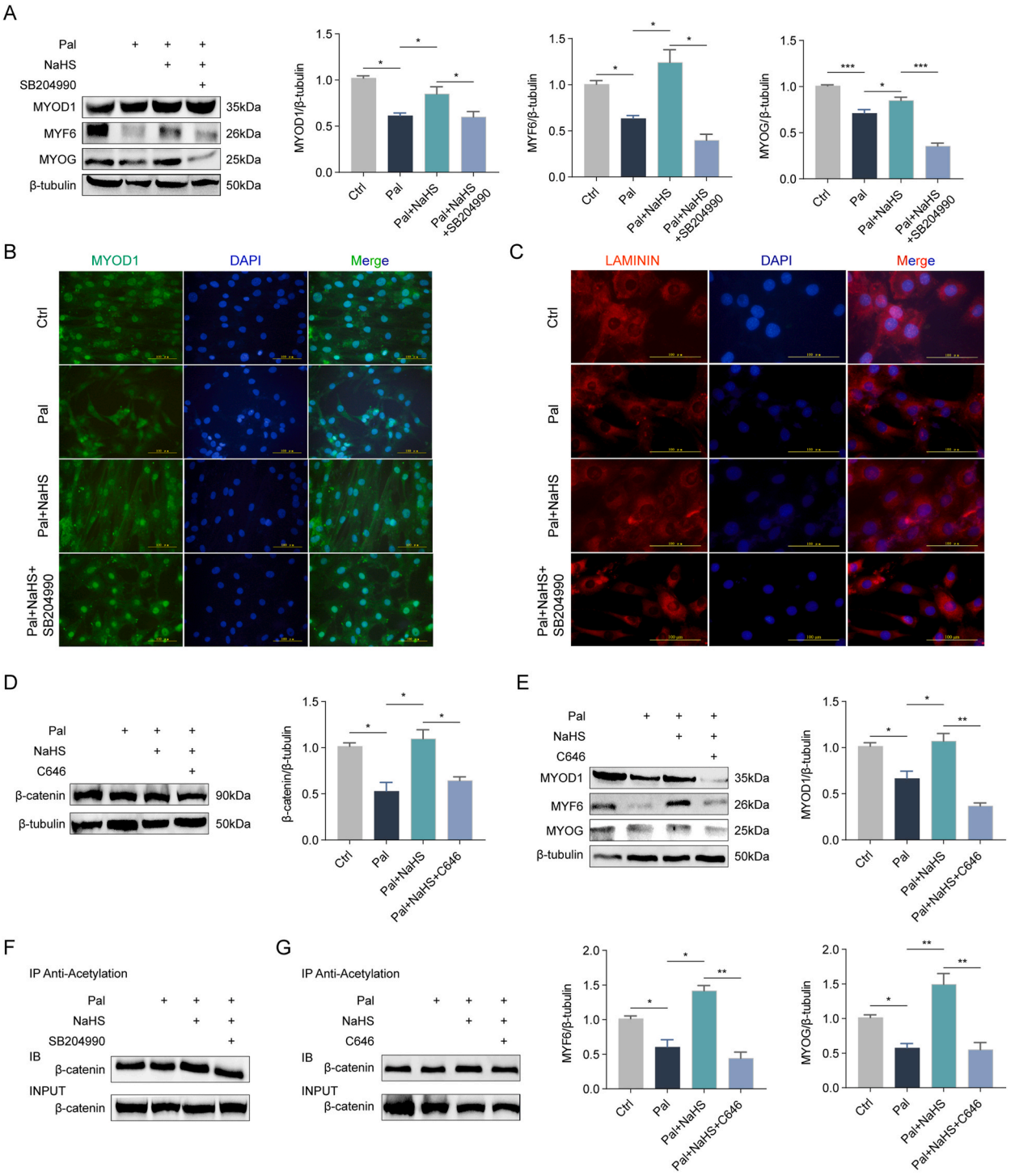

Fig. 4. Western blot was used to detect the expression levels of β-catenin and myogenic regulatory factors in the cytoplasm. (A) After the cells were treated with SB204990, the expression levels of myogenic regulatory factors were detected by Western blot. n = 4. (B) Immunofluorescence of MYOD1. (C) LAMININ staining was used to detect the differentiation of C2C12 myoblasts. (D) After the cells were treated with C646, the expression levels of β-catenin were detected by Western blot. n = 5. (E) After the cells were treated with C646, the expression levels of myogenic regulatory factors were detected by Western blot. n = 4. (F) After the cells were treated with SB204990, the interaction between β-catenin and acetylation by Co-immunocoprecipitation. (G) After the cells were treated with C646, the interaction between β-catenin and acetylation by Co-immunocoprecipitation. *P < 0.05, **P < 0.01, ***P < 0.001.

cells. Initially, we subjected these cells to 500 μM palmitate treatment for 48 h to investigate the presence of Reactive Oxygen Species (ROS) in the palmitate state. As depicted in Fig. S2A, ROS levels were elevated in the palmitate-treated group relative to the control group. Importantly, treatment with exogenous H_2S and NAC resulted in a reduction of ROS levels. We conducted Western blot analysis to assess the expression of SOD and CAT proteins and utilized SOD and CAT activity assays to measure their cytoplasmic activities. Our results indicated a significant decrease in both the protein levels and activities of SOD and CAT in the palmitate-treated group (Fig. 2D–E, and S2B). In summary, oxidative stress levels were heightened in the palmitate state compared to the control group, with exogenous H_2S and NAC effectively mitigating this oxidative stress condition.

3.3. Exogenous H_2S increased H_2S levels and CSE expression in C2C12 myoblasts

Previous studies have robustly established the prominent antioxidant properties of hydrogen sulfide (H_2S), with cystathionine-γ-lyase (CSE) and cystathionine-β-synthase (CBS) being central to cysteine production [17]. To ascertain H_2S levels, we utilized the H_2S probe 7-Azido-4-Methylcoumarin (C-7Az, 50 μmol/L). Our findings revealed a decrease in H_2S content in the palmitate-treated (pal) group relative to the control group. Intriguingly, upon the administration of exogenous H_2S, H_2S content increased, while it decreased in the palmitate + NaHS + PPG (a CSE inhibitor) group (Fig. 2F). Western blot was used to detect the expression of CSE, our results demonstrated that the expression of CSE was decreased in pal and Db/db group, whereas it was significantly increased after treatment with exogenous H_2S (Fig. 2G and H).

To further elucidate the underlying mechanism behind the diminished expression of CSE protein in the palmitate-treated group, we conducted a Co-immunoprecipitation experiment to assess the interaction between CSE and ubiquitin. Our results unveiled a significant augmentation in the interaction between CSE and ubiquitin in the palmitate-treated group. However, following treatment with exogenous H_2S or MG132 (a proteasome inhibitor), this interaction between CSE and ubiquitin was notably attenuated (Fig. 2I). In summation, our data indicates that exogenous H_2S plays a pivotal role in reducing the ubiquitination levels of CSE, thereby preserving CSE protein levels.

3.4. Exogenous H_2S promoted the differentiation of myoblasts in palmitate state

To explore the differentiation dynamics of C2C12 myoblasts in the presence of palmitate, we conducted Western blot analysis to assess the protein levels of MYOD1, MYF6, and MYOG. Our findings revealed a noteworthy reduction in the protein levels of MYOD1, MYF6, and MYOG in both the palmitate-treated (pal) and palmitate + NaHS + PPG (a CSE inhibitor) groups in comparison to the control group. However, upon administration of exogenous H_2S, the protein levels of MYOD1, MYF6, and MYOG exhibited a significant increase, as depicted in Fig. 3A. We used MYOD1 and MYOG staining to assess C2C12 myoblast differentiation under palmitate conditions. In Fig. 3B and C, we observed reduced MYOD1 and MYOG differentiation in the palmitate (pal) and palmitate with NaHS and PPG (pal + NaHS + PPG) groups compared to the control. Conversely, exogenous H_2S treatment resulted in longer muscle fibers, indicating increased differentiation.

The Wnt/β-catenin signaling pathway, a well-conserved pathway with pivotal roles in embryogenesis and organogenesis, has been implicated in muscle regeneration [10]. To investigate whether H_2S promotes myoblast differentiation under type 2 diabetes conditions, we assessed the levels of β-catenin protein. Our data unveiled a reduction in β-catenin protein levels in both the palmitate-treated and Db/db groups, while exogenous H_2S administration led to a noteworthy increase in β-catenin protein levels (Fig. 3D and E). Previous studies have highlighted p300-mediated acetylation of β-catenin, an event associated with the activation of the β-catenin signaling pathway through various mechanisms [13]. Our results indicated a significant reduction in total acetylation levels in the palmitate and palmitate + NaHS + PPG groups compared to the control and palmitate + NaHS groups (Fig. 3F). In conclusion, our findings suggest that exogenous H_2S enhances the acetylation levels of β-catenin, consequently mitigating its degradation.

3.5. Exogenous H_2S could increase the acetylation levels of β-catenin in the cytoplasm

Post-translational modifications play a crucial role in the regulation of β-catenin, with lysine residues being acetylated by acetyltransferases utilizing Acetyl-CoA as a cofactor. Acetyl-CoA synthesis is facilitated by ATP citrate lyase (ACLY), which converts citrate under ATP action into Acetyl-CoA [26]. To investigate the role of ACLY, we treated cells with the ACLY inhibitor SB204990 (100 μmol/L). Subsequently, Western blot analysis was conducted to assess the protein levels of MYOD1, MYF6, and MYOG. Our findings revealed that the protein levels of MYOD1, MYF6, and MYOG were elevated in the control and palmitate + NaHS groups compared to the palmitate-treated and palmitate + NaHS + SB204990 groups (Fig. 4A). MYOD1 staining was used to further verify the differentiation of C2C12 myoblasts after treatment with SB204990. Our results showed that the degree of differentiation of C2C12 myoblasts were again inhibited by treatment with SB204990 compared with exogenous H_2S treatment (Fig. 4B).

To further corroborate the impact of ACLY inhibition on C2C12 myoblast differentiation, we employed LAMININ staining. LAMININ staining was employed to assess the cross-sectional area of muscle fibers, revealing a reduction in cross-sectional area in the palmitate group, whereas the palmitate + NaHS group exhibited an increase, indicative of enhanced myoblast fusion. However, upon treatment with SB204990, myoblast fusion was notably reduced (Fig. 4C).

Acetylation of β-catenin by p300/CBP-associated factor (PCAF) enhances its interaction with cofactors and thereby boosts its transcriptional activity. To explore this further, C2C12 myoblasts were treated with the p300 inhibitor C646 (10 μmol/L), and Western blot analysis was employed to evaluate the levels of β-catenin and myogenic regulatory factors (MYOD1, MYF6, and MYOG). Our data

unveiled significantly lower protein levels of β-catenin and myogenic regulatory factors in the palmitate and palmitate + NaHS + C646 groups compared to the control and palmitate + NaHS groups (Fig. 4D–E). These observations suggest that exogenous NaHS enhances the cytoplasmic acetylation levels of β-catenin.

Building on the aforementioned results, we conducted Co-immunoprecipitation experiments to investigate the interaction between acetylated proteins and β-catenin. Our findings revealed a weakening of the interaction between acetylated proteins and β-catenin in the palmitate and palmitate + NaHS + C646 or palmitate + NaHS + SB204990 groups relative to the control group. Notably, treatment with NaHS resulted in an enhanced interaction between acetylated proteins and β-catenin (Fig. 4F–G). These results highlight the role of acetyl-CoA, under the action of p300, in acetylating lysine residues on β-catenin, thereby bolstering its transcriptional activity.

Given that palmitate is a 16C saturated fatty acid capable of mitochondrial β-oxidation, we examined the levels of PGC1-α protein, a critical regulator of mitochondrial biogenesis. Our results demonstrated significantly higher levels of PGC1-α protein in the palmitate + NaHS group compared to the palmitate and palmitate + NaHS + PPG groups (Fig. S3A). Mitochondrial membrane potential, assessed using the fluorescent probe JC-1, revealed a reduction in mitochondrial membrane potential (as indicated by the red-green fluorescence ratio) in the palmitate group relative to the control group. Notably, NaHS treatment led to an increase in mitochondrial membrane potential, while it decreased in the palmitate + NaHS + PPG group (Fig. S3B). These findings suggest that elevated palmitate levels negatively impact mitochondrial biogenesis and membrane potential.

3.6. Exogenous H_2S increased the levels of PKM1 protein

During glycolysis, glucose undergoes a series of metabolic transformations, ultimately yielding two pyruvate molecules. These pyruvate molecules subsequently enter the mitochondria, where they are converted into six-carbon citrate. This citrate is then

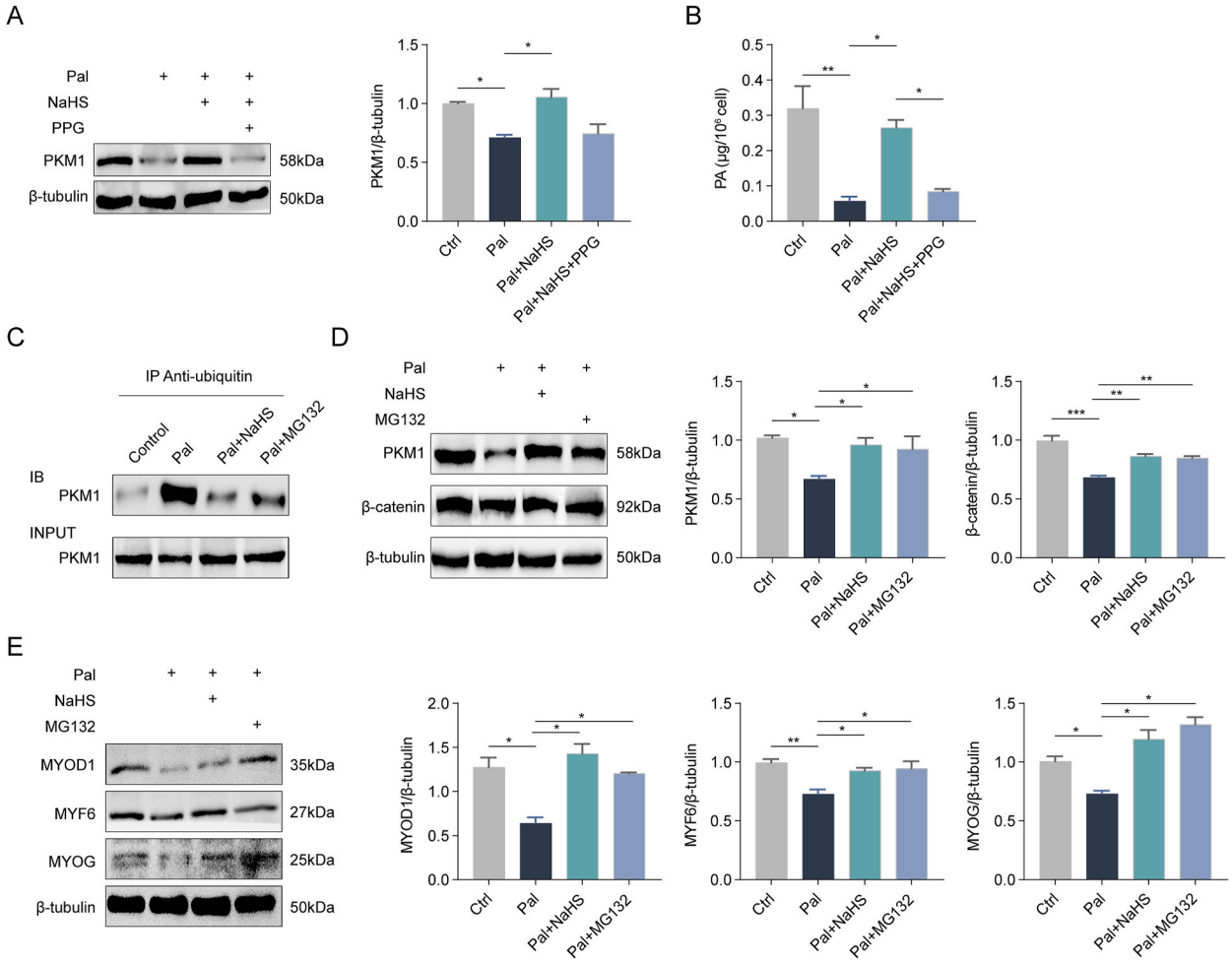

Fig. 5. Exogenous H_2S could increase the content of pyruvate in the cytoplasm. (A) The expression levels of PKM1 protein were detected by Western blot. n = 5. (B) Pyruvate (PA) content was detected by kit. n = 3. (C) The ubiquitination level of PKM1 was detected. (D) The expression levels of PKM1 and β-catenin were detected by Western blot. n = 5. (E) The expression levels of myogenic regulatory factors were detected by Western blot. n = 5. *P < 0.05, **P < 0.01, ***P < 0.001.

transported to the cytoplasm, where it participates in the regeneration of acetyl coenzyme A (acetyl-CoA) and oxaloacetate [27,28]. In the final step of glycolysis, pyruvate is converted, and the rate-limiting enzyme in this process is pyruvate kinase (PK). Hence, we examined the levels of PKM1 protein in our study. PKM1 expression displayed a decline in both the palmitate-treated (pal) and palmitate + NaHS + PPG (a CSE inhibitor) groups when compared to the palmitate + NaHS group (Fig. 5A). Correspondingly, the pyruvate content exhibited a decrease in the palmitate group, while it increased upon administration of exogenous H_2S (Fig. 5B). These findings imply a potential connection between PKM1 and the acetylation levels of β-catenin.

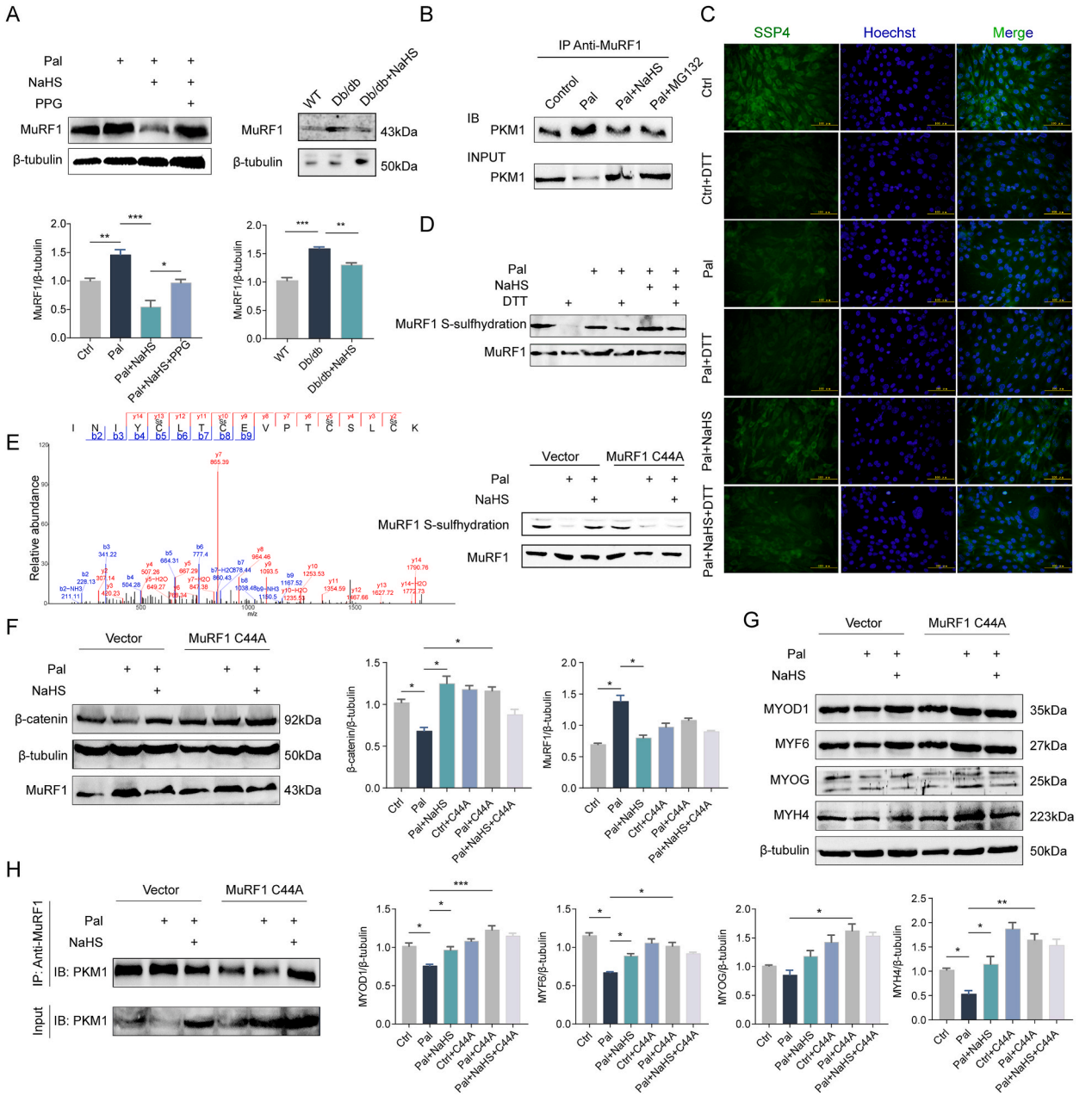

Fig. 6. Exogenous H_2S regulated MuRF1 through S-sulfhydration modification, and then promoted the differentiation of C2C12 myoblasts. (A) The expression level of MuRF1 was detected by Western blot. n = 5. (B) The interaction between PKM1 and MuRF1 was detected by Co-immunoprecipitation. (C) The levels of intracellular S-sulfhydration were detected by fluorescent probe SSP4. (D) The S-sulfhydration modification of MuRF1 by Biotin assays. (E) Mass spectrometry identified the S-sulfhydration modification sites on cysteine residues of MuRF1 (left panel). After transfection of MuRF1 Cys44 mutants for 24 h, the S-sulfhydration modification of MuRF1 (right panel). (F) After transfection of MuRF1 Cys44 mutants for 24 h,the expressions of MuRF1、β-catenin were detected by Western blot. n = 5. (G) After transfection of MuRF1 Cys44 mutants for 24 h, the expressions of myogenic regulatory factors and MYH4 were detected by Western blot. n = 5. (H) After MuRF1 Cys44 mutants were transfected for 24 h, the interaction between MuRF1 and PKM1 was detected by Co-immunoprecipitation. *P < 0.05, **P < 0.01, ***P < 0.001.

To elucidate the underlying mechanism behind the reduction in PKM1 expression, we conducted a Co-immunoprecipitation experiment to explore the interaction between PKM1 and ubiquitin. As depicted in Fig. 5C, the interaction between PKM1 and ubiquitin was markedly higher in the palmitate group in comparison to the control, palmitate + NaHS, and palmitate + MG132 (a proteasome inhibitor) groups. Subsequent Western blot analysis revealed diminished protein levels of both PKM1 and β-catenin in the palmitate group compared to the control, palmitate + NaHS, and palmitate + MG132 groups (Fig. 5D). Furthermore, we observed a reduction in the protein levels of myogenic regulatory factors (MYOD1, MYF6, MYOG) in the palmitate group relative to the control group. Notably, treatment with both MG132 and NaHS restored the levels of myogenic regulatory factors (Fig. 5E). These results collectively underscore the role of the ubiquitin-proteasome system in mediating the decreased expression of PKM1 in the palmitate-treated group, subsequently impacting the expression of myogenic regulatory factors.

3.7. Exogenous H_2S regulated MuRF1 through S-sulfhydration modification and promoted the differentiation of C2C12 myoblasts

To elucidate the mechanism underlying the reduction of PKM1 protein levels in the palmitate-treated (pal) group, we examined the expression of MuRF1, an E3 ligase enzyme. Our results in Fig. 6A showed an increase in MuRF1 protein levels in the pal and Db/db group compared to the control group. Interestingly, the administration of exogenous H_2S led to a reduction in MuRF1 protein levels. These observations suggested a potential link between the elevated MuRF1 levels, acting as an E3 ligase, in the pal group and the decrease in PKM1 protein levels. In Fig. 6B, we observed an increased interaction between MuRF1 and PKM1 in the pal group compared to the control group. However, following treatment with exogenous H_2S and MG132, this interaction between MuRF1 and PKM1 was reduced.

Considering the observed increase in ubiquitination levels and oxidative stress in the pal group, we speculated that alterations in the redox state may impact protein folding homeostasis, potentially leading to the accumulation of unfolded proteins and endoplasmic reticulum (ER) stress [29]. Consequently, we assessed the expression levels of proteins related to the ER stress pathway (p-PERK/PERK, ATF4, Chop) and Bip. We observed significant upregulation of these ER stress-related proteins in both the pal and Control + Tg groups. However, treatment with 4-phenylbutyric acid (4-PBA, an ER stress inhibitor) and NaHS led to a decrease in the levels of these ER stress-related proteins (Fig. S4).

Accumulating evidence suggests that H_2S can modify target proteins through S-sulfhydration, influencing their activity [30]. Thus, we further explored whether H_2S could regulate the expression of MuRF1 protein via S-sulfhydration modification under palmitate conditions. We employed the fluorescent probe SSP4 to detect intracellular S-sulfhydration production. Notably, S-sulfhydration production was reduced in the pal group but increased following exogenous H_2S administration. Treatment with dithiothreitol (DTT), a disulfide bond inhibitor, diminished the S-sulfhydration of MuRF1 (Fig. 6C). Furthermore, Biotin Assay analysis demonstrated that H_2S could regulate MuRF1 through S-sulfhydration, whereas DTT attenuated the S-sulfhydration of MuRF1 (Fig. 6D). Specifically, we found that H_2S could modify the Cys44 site of MuRF1 via S-sulfhydration (Fig. 6E).

To further explore whether H_2S, through S-sulfhydration modification of MuRF1, could promote the differentiation of C2C12 myoblasts, we transfected MuRF1 Cys44 mutants into C2C12 myoblasts. These cells were also treated with palmitate and NaHS to assess the levels of MuRF1, β-catenin, myogenic regulatory factors (MYOD1, MYF6, MYOG), and MYH4. Fig. 6F–G indicated that the protein levels of MuRF1 in the pal group were higher than those in the control and palmitate + NaHS groups. Notably, the protein levels of β-catenin, myogenic regulatory factors, and MYH4 were decreased in the pal group. However, upon transfection with MuRF1 Cys44 mutants, the protein levels of β-catenin, myogenic regulatory factors, and MYH4 were increased. These results suggest that H_2S, through S-sulfhydration modification of MuRF1, not only elevates β-catenin levels but also enhances the levels of myogenic regulatory factors and MYH4, ultimately promoting the differentiation of C2C12 myoblasts.

Our findings collectively establish that H_2S can modulate MuRF1 through S-sulfhydration modification, and this modification occurs at the Cys44 site of MuRF1. To further elucidate the regulatory role of MuRF1 in the interaction with PKM1, we conducted a Co-immunoprecipitation experiment. Fig. 6H demonstrates that the interaction between MuRF1 and PKM1 was significantly higher in the pal group compared to the control and NaHS groups. However, the interaction between MuRF1 and PKM1 was attenuated following the transfection of MuRF1 Cys44 mutants into C2C12 myoblasts. Our data underscore that MuRF1 interacts with PKM1, thereby regulating the expression of myogenic regulatory factors.

4. Discussion

In this study, we found that (1) H_2S levels and the levels of CSE protein were decreased in pal group. (2) Exogenous H_2S promoted the expression levels of myogenic regulatory factors (MYOD1, MYF6, MYOG) and myoblasts differentiation. (3) Exogenous H_2S increased the expression levels of PKM1 by S-sulfhydration modification of MuRF1. These findings collectively suggest that exogenous H_2S holds therapeutic potential for attenuating skeletal muscle atrophy in type 2 diabetes. In skeletal muscle, satellite cells reside in a quiescent state characterized by low metabolic demands and limited mitochondrial content. These resting muscle satellite cells primarily rely on glucose and fatty acid oxidation, as well as glycolysis, which results in reduced levels of histone acetylation due to the limited availability of acetyl-CoA. Concurrently, higher levels of NAD boost SIRT1 activity, facilitating histone deacetylation. Fig. 3F underscores this observation by depicting a decrease in acetylation levels in the pal group compared to the pal + NaHS group. Upon activation, satellite cells undergo mitochondrial biogenesis and increase glycolysis, which is accompanied by a reduction in histone acetylation. As satellite cells enter mitosis and experience mitochondrial fission, mitochondrial capacity decreases, consequently elevating glucose dependence [31].

Furthermore, our study revealed a decrease in the levels of Peroxisome Proliferator-Activated Receptor Gamma Coactivator 1-

Alpha (PGC1-α) protein and a decrease in mitochondrial membrane potential in the pal group (Figs. S3A–B). The treatment of myoblasts with 500 μmol/L of palmitate caused significant alterations in mitochondrial biogenesis and membrane potential. Notably, even in the presence of palmitate, mitochondrial β-oxidation and acetyl-CoA production were compromised.

The loss of skeletal muscle mass is associated with reduced physical activity, leading to increased mortality. Among the four main endogenous protein degradation systems in vertebrates, the Ubiquitin-Proteasome System (UPS) plays a pivotal role in regulating skeletal muscle quality and regeneration. UPS comprises three key components: Ubiquitin E1 (activating enzyme), Ubiquitin E2 (conjugating enzyme), and Ubiquitin E3 (ligase enzyme). Muscle-specific RING-type E3 ligase (MuRF1) belongs to the E3 ligase family and is a reliable marker of skeletal muscle atrophy [32]. MuRF1 and MuRF2 regulate glucose and fat metabolism, with MuRF1 potentially being a target for preventing muscle weakness in type 2 diabetes mellitus [33–35]. While MuRF1's role in the degradation of myofilament proteins in skeletal muscle has been documented, there has been limited research elucidating the mechanism by which MuRF1 promotes myoblast differentiation. Our study revealed an increase in MuRF1 expression and an enhanced interaction between MuRF1 and PKM1 in the pal group, leading to a decrease in PKM1 protein levels (Fig. 6B). It's noteworthy that PKM1, one of the four PKM isoforms in mammals, is predominantly expressed in skeletal muscle, smooth muscle, and the brain [36]. Previous research indicates that PKM1 tends to favor oxidative phosphorylation [37] and may promote tumor cell growth [38]. The reduced PKM1 protein levels in the pal group corresponded to a decrease in oxidative phosphorylation levels. This decrease in PKM1 levels ultimately led to reduced β-catenin acetylation and its subsequent degradation via the ubiquitin-proteasome pathway.

The Wnt/β-catenin signaling pathway plays a pivotal role in the transition from quiescent satellite cells to differentiated muscle fibers [39]. Canonical Wnt signaling induces the expression of myogenic factors such as Myf5 and MyoD in somites/sarcomeres, thus promoting embryonic myogenesis [40]. Several studies have demonstrated that Wnt ligands can enhance myoblast differentiation in vitro [41,42] and increase the expression of MyoD and MYOG [43,44]. Kim et al. found that β-catenin can interact with MyoD, enhancing MyoD's ability to bind and activate target genes in C2C12 myoblasts [45]. Cui et al. disrupted C2C12 myoblast differentiation through β-catenin knockout, further supporting the notion that β-catenin promotes C2C12 myoblast differentiation [46]. Building upon these insights and considering the competitive relationship between acetylation and ubiquitination at the same lysine residues, our study focused on β-catenin acetylation as a potential regulatory mechanism. Our results demonstrated an increase in the interaction between β-catenin and acetylated proteins in the control group, a decrease in this interaction in the pal group, and an association between mitochondrial dysfunction and reduced acetylation levels (Fig. 4F and G). Our study was primarily centered on the later stages of myoblast differentiation, during which mitochondrial activity supplies acetyl-CoA. Reduced mitochondrial biogenesis and membrane potential were observed in the pal group due to mitochondrial dysfunction. This, in turn, reduced Acetyl-CoA levels. Our experiments further confirmed the significance of β-catenin acetylation in the expression of myogenic regulatory factors, as treatment with ATP citrate lyase inhibitor SB204990 and p300 inhibitor C646 resulted in decreased expression of these factors (Fig. 4A and E). This novel perspective on myoblast differentiation underscores the critical role of β-catenin acetylation. In summary, our investigation provides compelling evidence that exogenous H_2S enhances S-sulfhydration at the Cys44 site of MuRF1. This modification effectively regulates PKM1 protein levels, augments the expression of myogenic regulatory factors, and fosters myoblast differentiation within a high-palmitate environment (Fig. S5).

5. Conclusions

In summary, our study reveals that hydrogen sulfide (H_2S) regulate the Wnt signaling pathway to alleviate skeletal muscle atrophy in type 2 diabetes. These findings offer new insights into potential therapeutic targets for treating this condition.

Data availability statement

The data associated with this study have not been deposited in a publicly available repository. The data can be made available upon request. Please contact the corresponding author for more information.

CRediT authorship contribution statement

Fangping Lu: Writing – original draft, Methodology, Data curation. **Shiwu Zhang:** Visualization, Methodology, Investigation. **Shiyun Dong:** Formal analysis, Data curation. **Mengyi Wang:** Validation, Investigation. **Kemiao Pang:** Investigation, Formal analysis. **Yajun Zhao:** Supervision, Conceptualization. **Jiayi Huang:** Visualization, Validation. **Jiaxin Kang:** Methodology, Data curation. **Ning Liu:** Methodology. **Xueya Zhang:** Visualization, Methodology, Data curation. **Dechao Zhao:** Investigation, Formal analysis. **Fanghao Lu:** Supervision, Methodology, Formal analysis. **Weihua Zhang:** Validation, Supervision, Formal analysis.

Declaration of competing interest

The authors declare no conflict of interest.

Grants

This work was supported by the National Natural Science Foundation of China (No.82270359, 82370367).

Appendix A. Supplementary data

Supplementary data to this article can be found online at https://doi.org/10.1016/j.heliyon.2024.e38661.

References

[1] K.F. Petersen, G.I. Shulman, Pathogenesis of skeletal muscle insulin resistance in type 2 diabetes mellitus, Am. J. Cardiol. 90 (5A) (2002) 11G–18G.
[2] L. Goth, Catalase deficiency and type 2 diabetes 31 (12) (2008) e93.
[3] S. Kuang, M.A. Rudnicki, The emerging biology of satellite cells and their therapeutic potential, Trends Mol. Med. 14 (2008) 82–91.
[4] S.B. Charge, M.A. Rudnicki, Cellular and molecular regulation of muscle regeneration, Physiol. Rev. 84 (2004) 209–238.
[5] P.S. Zammit, J.P. Golding, Y. Nagata, V. Hudon, T.A. Partridge, J.R. Beauchamp, Muscle satellite cells adopt divergent fates: a mechanism for self-renewal? J. Cell Biol. 166 (2004) 347–357.
[6] P.S. Zammit, F. Relaix, Y. Nagata, A.P. Ruiz, C.A. Collins, T.A. Partridge, J.R. Beauchamp, Pax7 and myogenic progression in skeletal muscle satellite cells, J. Cell Sci. 119 (2006) 1824–1832.
[7] M.H. Nguyen, M. Cheng, T.J. Koh, Impaired muscle regeneration in ob/ob and db/db mice, Sci. World J. 11 (2011) 1525–1535.
[8] Kuo Zhang, Yuying Zhang, Lijie Gu, Miaomiao Lan, Chuncheng Liu, Meng Wang, Yang Su, Mengxu Ge, Tongtong Wang, Yingying Yu, Chang Liu, Li Lei, Qiuyan Li, Yaofeng Zhao, Zhengquan Yu, Islr regulates canonical Wnt signaling-mediated skeletal muscle regeneration by stabilizing Dishevelled-2 and preventing autophagy, Nat. Commun. 9 (2018) 5129.
[9] Abhinav Adhikari, Judith Davie, JARID2 and the PRC2 complex regulate skeletal muscle differentiation through regulation of canonical Wnt signaling, Epigenet Chromatin. 11 (2018) 46.
[10] Francesco Girardi, Fabien Le Grand, Wnt signaling in skeletal muscle development and regeneration, Progr. Mol. Biol. Transl. Sci. (2018) 157–179.
[11] C. Gao, G. Xiao, J. Hu, Regulation of Wnt/β-catenin signaling by posttranslational modifications, Cell Biosci. 4 (2014) 13.
[12] Mary C. Sugden, Mark J. Holness, The pyruvate carboxylase-pyruvate dehydrogenase axis in islet pyruvate metabolism: going round in circles, Islets 3 (6) (2011) 302–319.
[13] Brianna H. Shares, Melanie Busch, Noelle White, X Laura Shum, X. Roman A. Eliseev, Active mitochondria support osteogenic differentiation by stimulating β-catenin acetylation, J. Biol. Chem. 293 (41) (2018) 16019–16027.
[14] Fangping Lu, Baoling Lu, Linxue Zhang, JingChen Wen, Mengyi Wang, Shiwu Zhang, Qianzhu Li, Feng Shu, Yu Sun, Ning Liu, Shuo Peng, Yajun Zhao, Shiyun Dong, Hydrogen sulphide ameliorating skeletal muscle atrophy in db/db mice via Muscle RING finger 1 S-sulfhydration, J. Cell Mol. Med. 00 (2020) 1–16.
[15] M. Mrosek, S. Meier, Z. Ucurum-Fotiadis, E. von Castelmur, E. Hedbom, A. Lustig, S. Grzesiek, D. Labeit, S. Labeit, O. Mayans, Structural analysis of B-Box 2 from MuRF1: identification of a novel self-association pattern in a RING-like fold, Biochemistry 47 (2008) 10722–10730.
[16] Qing Xiao, Jiayi Ying, Leihong Xiang, Chengfeng Zhang, The biologic effect of hydrogen sulfide and its function in various diseases, Medicine (Baltim). 97 (44) (2018) e13065.
[17] P.K. Chakraborty, X. Xiong, S.B. Mustafi, S. Saha, D. Dhanasekaran, N.A. Mandal, S. McMeekin, R. Bhattacharya, P. Mukherjee, Role of cystathionine beta synthase in lipid metabolism in ovarian cancer, Oncotarget 6 (2015) 37367–37384.
[18] N.L. Kanagy, C. Szabo, A. Papapetropoulos, Vascular biology of hydrogen sulfide, Am. J. Physiol. Cell Physiol. 312 (2017) C537–C549.
[19] Z.Z. Zhao, Z. Wang, G.H. Li, R. Wang, J.M. Tan, X. Cao, R. Suo, Z.S. Jiang, Hydrogen sulfide inhibits macrophage-derived foam cell formation, Exp. Biol. Med. 236 (2011) 169–176.
[20] C. Wang, J. Du, S. Du, Y. Liu, D. Li, X. Zhu, X. Ni, Endogenous H_2S resists mitochondria-mediated apoptosis in the adrenal glands via ATP5A1 S-sulfhydration in male mice, Mol. Cell. Endocrinol. 474 (2018) 65–73.
[21] A. Ahmad, C. Szabo, Both the H_2S biosynthesis inhibitor aminooxyacetic acid and the mitochondrially targeted H_2S donor AP39 exert protective effects in a mouse model of burn injury, Pharmacol. Res. 113 (2016) 348–355.
[22] M.R. Filipovic, Persulfidation (S-sulfhydration) and H_2S, Handb. Exp. Pharmacol. 230 (2015) 29–59.
[23] Asif K. Mustafa, Moataz M. Gadalla, Nilkantha Sen, Seyun Kim, Weitong Mu, Sadia K. Gazi, Roxanne K. Barrow, Guangdong Yang, Rui Wang, Solomon H. Snyder, H_2S signals through protein S-sulfhydration, Sci. Signal. 2 (2009) ra72.
[24] Changyuan Lu, Adam Kavalier, Eugene Lukyanov, Steven S. Gross, S-sulfhydration/desulfhydration and S-nitrosylation/denitrosylation: a common paradigm for gasotransmitter signaling by H_2S and No, Methods 62 (2) (2013) 177–181.
[25] V. Renault, L.-E. Thorne, P.-O. Eriksson, G. Butler-Browne, V. Mouly, Regenerative potential of human skeletal muscle during aging, Aging Cell (2002) 132–139.
[26] Adrian Drazic, Line M. Myklebust, Rasmus Ree, Thomas Arnesen, The world of protein acetylation, Biochim. Biophys. Acta 1864 (10) (2016) 1372–1401.
[27] F.L. Theodoulou, O.C. Sibon, S. Jackowski, I. Gout, Coenzyme A and its derivatives: renaissance of a textbook classic, Biochem. Soc. Trans. 42 (2014) 1025–1032.
[28] Monica Dominguez, Bernhard Brüne, Dmitry Namgaladze, Exploring the role of ATP-citrate lyase in the immune system, Front. Immunol. 12 (2021) 632526.
[29] H.M. Zeeshan, G.H. Lee, H.R. Kim, H.J. Chae, Endoplasmic reticulum stress and associated ROS, Int. J. Mol. Sci. 17 (2016) 327.
[30] C. Szabo, Hydrogen sulfide, an enhancer of vascular nitric oxide signaling: mechanisms and implications, Am. J. Physiol. Cell Physiol. 312 (2017) C3–C15.
[31] Nora Yucel, Yu Xin Wang, Thach Mai, Sean C. Bendall, Michael Angelo, Helen M. Blau, Glucose metabolism drives histone acetylation landscape transitions that dictate muscle stem cell function, Cell Rep. 27 (2019) 3939–3955.
[32] S.H. Lecker, R.T. Jagoe, A. Gilbert, M. Gomes, V. Baracos, J. Bailey, S.R. Price, W.E. Mitch, A.L. Goldberg, Multiple types of skeletal muscle atrophy involve a common program of changes in gene expression, FASEB J. 18 (2004) 39–51.
[33] S. Hirner, C. Krohne, A. Schuster, S. Hoffmann, S. Witt, R. Erber, C. Sticht, A. Gasch, S. Labeit, D. Labeit, MuRF1-dependent regulation of systemic carbohydrate metabolism as revealed from transgenic mouse studies, J. Mol. Biol. 379 (4) (2008 Jun 13) 666–677.
[34] S.H. Witt, H. Granzier, C.C. Witt, S. Labeit, MURF-1 and MURF-2 target a specific subset of myofibrillar proteins redundantly: towards understanding MURF-dependent muscle ubiquitination, J. Mol. Biol. 350 (4) (2005 Jul 22) 713–722.
[35] S. Labeit, S. Hirner, J. Bogomolovas, A. Cruz, M. Myrzabekova, A. Moriscot, T.S. Bowen, V. Adams, Regulation of glucose metabolism by MuRF1 and treatment of myopathy in diabetic mice with small molecules targeting MuRF1, Int. J. Mol. Sci. 22 (4) (2021 Feb 23) 2225.
[36] L Dayton Talya, Jacks Tyler, Matthew G Vander Heiden, PKM2, cancer metabolism, and the road ahead, EMBO Rep. 17 (12) (2016) 1721–1730.
[37] Gaochao Dong, Qixing Mao, Wenjie Xia, Youtao Xu, Jie Wang, Xu Lin, Feng Jiang, PKM2 and cancer: the function of PKM2 beyond glycolysis, Oncol. Lett. 11 (2016) 1980–1986.
[38] Mami Morita, Taku Sato, Miyuki Nomura, Yoshimi Sakamoto, Yui Inoue, Ryota Tanaka, Shigemi Ito, Koreyuki Kurosawa, Kazunori amaguchi, YukiSugiura, Hiroshi Takizaki, Yoji Yamashita, Ryuichi Katakura, Ikuro Sato, Masaaki Kawai, Yoshinori Okada, Hitomi Watanabe, GenKondoh, Shoko Matsumoto, Ayako Kishimoto, Miki Obata, Masaki Matsumoto, Tatsuro Fukuhara, Hozumi Motohashi, Makoto Suematsu, Masaaki Komatsu, Keiichi I. Nakayama, Toshio Watanabe, Tomoyoshi Soga, Hiroshi Shima, Makoto Maemondo, Nobuhiro Tanuma, PKM1 confers metabolic advantages and promotes cell-autonomous tumor cell growth, Cancer Cell. 33 (2018) 355–367.e7.
[39] C. Florian Bentzinger, Yu Xin Wang, Michael A. Rudnicki, Building muscle: molecular regulation of myogenesis, Cold Spring Harb. Perspect. Biol. 4 (2) (2012) a008342.
[40] J. Von Maltzahn, N.C. Chang, C.F. Bentzinger, M.A. Rudnicki, Wnt signaling in myogenesis, Trends Cell Biol. 22 (11) (2012) 602–609.

[41] N. Pansters, J. van der Velden, M. Kelders, H. Laeremans, A. Schols, R. Langen, Segregation of myoblast fusion and muscle-specific gene expression by distinct ligand-dependent inactivation of GSK-3β, Cell. Mol. Life Sci. 68 (3) (2011) 523–535.
[42] A.S. Brack, I.M. Conboy, M.J. Conboy, J. Shen, T.A. Rando, A temporal switch from notch to Wnt signaling in muscle stem cells is necessary for normal adult myogenesis, Cell Stem Cell. 2 (1) (2008) 50–59.
[43] A.G. Ridgeway, H. Petropoulos, S. Wilton, I.S. Skerjanc, Wnt signaling regulates the function of MyoD and myogenin, J. Biol. Chem. 275 (42) (2000) 32398–32405.
[44] H. Petropoulos, I.S. Skerjanc, Beta-catenin is essential and sufficient for skeletal myogenesis in P19 cells, J. Biol. Chem. 277 (18) (2002) 15393–15399.
[45] C.-H. Kim, H. Neiswender, E.J. Baik, W.C. Xiong, L. Mei, Beta - catenin interacts with MyoD and regulates its transcription activity, Mol. Cell Biol. 28 (9) (2008) 2941–2951.
[46] Shuang Cui, Liang Li, Ruth T. Yu, Michael Downes, Ronald M. Evans, Julie-Ann Hulin, Helen P. Makarenkova, Robyn Meech, β-catenin is essential for differentiation of primary myoblasts via cooperation with MyoD and α-catenin, Development 146 (6) (2019) dev167080.